JOURNAL OF PROPULSION AND POWER
Vol. 11, No. 4, July–August 1995

# High-Performance Propellants Based on Hydrazinium Nitroformate

H. F. R. Schöyer* and A. J. Schnorhk†
*ESA/ESTEC, 2200 AG Noordwijk, The Netherlands*
P. A. O. G. Korting‡ and P. J. van Lit§
*Aerospace Propulsion Products, 4600 AR Bergen op Zoom, The Netherlands*
and
J. M. Mul,¶ G. M. H. J. L. Gadiot,** and J. J. Meulenbrugge††
*Prins Maurits Laboratory TNO, 2280 AA Rijswijk, The Netherlands*

**The identification of potential high-performance propellant combinations is based on a fundamental analysis of the governing parameters. Its development requires the establishment of its safety and handling characteristics and its thermodynamic decomposition and explosive properties. After the identification of hydrazinium nitroformate (HNF) as a promising new oxidizer, the development of a new composite solid propellant based on HNF and energetic binders such as glycidyl azide polymer (GAP), poly 3,3-bis(azidomethyl)oxetane, poly 3-nitromethoxy-3-methyl oxetane (polynimmo), or poly glycidyl nitrate (polyglyn) was started. A pilot plant for the production of HNF has been constructed and many of the properties of HNF and HNF/aluminum (Al)/GAP propellants have been established. Initial development tests show that HNF looks suitable as a propellant oxidizer, while initial tests with HNF/Al/GAP confirm the expected increase in performance over existing composite propellants. Impact and friction sensitivity have been determined for HNF and HNF-based propellants. Areas that are still open for investigation are also addressed. This article gives a comprehensive overview of the status of this development.**

## Nomenclature

$A$ = surface area
$C_p$ = heat capacity at constant pressure
$c^*$ = characteristic velocity
$H$ = enthalpy
$I$ = impulse
$M$ = mass
$\mathcal{M}$ = molar mass
$n$ = number of mol
$p$ = pressure
$R_0$ = universal gas constant, 8.31434 J/mol·K
$T$ = temperature
$V$ = volume
$v$ = velocity
$x$ = crystal size
$\gamma$ = ratio of specific heats
$\Delta$ = increment
$\varepsilon$ = expansion ratio, $A_e/A_t$
$\rho$ = density
$\langle\ \rangle$ = mean value

*Subscripts*
$c$ = combustion, chamber conditions
$e$ = exit
$f$ = formation
$p$ = propellant
sp = specific
$t$ = throat
vac = vacuum conditions
$\delta$ = density
0 = initial conditions

*Superscript*
0 = standard conditions

## I. Introduction

THE development of a new composite propellant requires much time and effort. The development of hydroxy terminated polybutadiene (HTPB) as a rocket propellant binder took about 17 years from the initial research and development until its use in an operational system.[1]

After the European Space Agency (ESA), and the Netherlands Agency for Aerospace Programs (NIVR) had identified the propellant combination hydrazinium nitroformate/aluminum/glycidyl azide polymer (HNF/Al/GAP) as a very promising high-performance propellant,[2] the development work on this new propellant was started in 1988. The identified propellant has two distinct advantages: 1) a much higher specific impulse than any of the existing solid propellants and 2) chlorine-free exhaust products. The latter is especially important in view of the concern about damage to the ozone layer due to launches by solid rocket motors.

The governing rocket performance parameters and various potential propellant combinations were systematically considered. Subsequently, a detailed search was initiated to find combinations of potential oxidizers and binders that met the requirement of maximizing the specific impulse. A number of potential oxidizers and binders were found. The selection of those with which to proceed depends not only on the predicted performance increase, but also on the availability of ingredients, and the possibility of safe handling and manu-

---

Received July 5, 1994; revision received Oct. 21, 1994; accepted for publication Dec. 13, 1994.

*Senior Propulsion Engineer for Special Assignments, P.O. Box 299. Senior Member AIAA.

†Propulsion Engineer, P.O. Box 299. Member AIAA.

‡Managing Director, P.O. Box 697. Member AIAA.

§Process Engineer, P.O. Box 697.

¶Research Chemist, P.O. Box 45. Member AIAA.

**Propulsion Engineer, P.O. Box 45.

††Head Research Group Pyrotechnics and Energetic Materials, P.O. Box 45.

facturing. There should be some indication that the production of such a propellant in the future might be economically attractive. Also, no combinations should be used that might pose severe environmental or health constraints. For example, while beryllium and fluorine compounds may lead to propellants with very attractive performance characteristics, such combinations were ruled out from the start. Even if the environmental hazard for space use might be acceptable, it was felt that ground testing and manufacturing might pose insurmountable difficulties.

The selection of the combination on which to concentrate for further development work was primarily determined by the availability of ingredients and materials. Two oxidizers seemed to be of most interest: ammonium dinitramide (ADN) and HNF, whereas the identified binders: poly 3,3-bis(azidomethy)oxetane [BAMO], GAP, poly 3-nitromethoxy-3-methy oxetane (polynimmo) [PLN], and poly glycidyl nitrate (polyglyn) [PGN] all seemed to lead to very promising combinations. In the meantime, another oxidizer, CL20, has emerged. This oxidizer was not considered because there is no detailed information about its thermodynamic properties known to the authors. However, it is highly deficient in oxygen, like hexogen (RDX) and octogen (HMX). On the other hand, ADN and HNF were already known, although the information on ADN was rather limited. In some respects HNF looked more attractive than ADN.

While four different energetic binders were identified, only GAP was available on a commercial basis at the time of selection. This was a major reason to select GAP over any of the other potential binders. It is believed that the development of an HNF propellant combination with another binder could take place in a later or parallel phase, once these binders become available commercially.

There was no commercial HNF production, therefore, the manufacturing process and synthesis route of HNF had to be investigated and quality control procedures had to be established and implemented. After the successful laboratory production of HNF, a bench-scale production was set up. The results of this production were so encouraging that a pilot plant for the production of HNF has been built. This plant is now operational.

HNF and HNF-based propellants exhibit very high burning rate exponents, close to unity. While for some applications the high burning rate exponent may be attractive, one needs lower burning rate exponents for use in rocket motors. Based upon the decomposition characteristics of HNF, it is believed that suitable burning rate modifiers can be identified. Presently, this aspect of the development is still open, although there have been reports that burning rate exponents close to 0.5 have been realized.[3]

Another aspect is that, under normal production, as realized under laboratory conditions and in the pilot plant, HNF tends to form needle-like crystals. This crystal shape hampers a high solid loading in GAP propellants. Presently, work is under way to obtain more spherical- or cubical-shaped crystals. These results look extremely promising.

To obtain a qualifiable rocket propellant, it is mandatory to be able to polymerize the binder in combination with the oxidizer and aluminium. Although a curing system and procedure have been developed that allow one to obtain cured propellant samples, more work is necessary to arrive at propellants that will meet all requirements with regard to mechanical properties and storage life. At present, no efforts have been made in determining any mechanical property of the propellants; mainly because the amount of propellant that has been produced until now was too small, but also because the primary objective of the present development effort is to demonstrate in actual tests the expected increase in specific impulse.

The development work on HNF-based composite propellants is far from complete, but the results until now all seem to indicate that it will be possible to make a qualifiable composite solid propellant yielding a significant increase in performance.

## II. How to Achieve More Performing Propellants

### A. Fundamental Aspects

Tsiolkovky's equation gives the velocity increment of a rocket stage as[4]

$$\Delta v = I_{\mathrm{sp}} \cdot \log_e[M_0/(M_0 - M_p)] \tag{1}$$

Here, $\Delta v$ stands for the velocity increment of a stage, $M_0$ stands for the initial mass of the stage, and $M_p$ for the propellant mass of the stage. To maximize performance, one may maximize the ratio $M_p/M_0$, or try to increase the specific impulse $I_{\mathrm{sp}}$. The specific impulse $I_{\mathrm{sp}}$ is given by[4]

$$I_{\mathrm{sp}} = \sqrt{[2\gamma/(\gamma - 1)](R_0/\mathcal{M})T_c[1 - (p_e/p_c)^{(\gamma-1)/\gamma}]} \tag{2}$$

It depends on engine properties, i.e., the ratio of exit and combustion pressure, and on the properties of the combustion gases: the molar mass $\mathcal{M}$ of the combustion products, the ratio of specific heats $\gamma$, and the combustion temperature $T_c$.

The molar mass of the combustion products shall be as low as possible, which favors propellants that contain many of the lighter elements, like hydrogen. The ratio of specific heats shall be as high as possible. This implies a small value of the heat capacity, $C_p$. These quantities are related by

$$C_p = [\gamma/(\gamma - 1)](R_0/\mathcal{M}) \tag{3}$$

The lowest values for $C_p$ are found for monoatomic gases; polyatomic gases have a higher $C_p$. Some typical values for $C_p$ in rocket motor combustion gases are given in Table 1.

The combustion temperature results from the energy release during the combustion, i.e., the heat of reaction and specific heat of the combustion products:

$$T_c = -\Delta H/C_p \tag{4}$$

The heat of reaction $\Delta H$ follows from

$$\Delta H(T) = \sum [n\Delta H_f^0(T)]_{\mathrm{products}} - \sum [n\Delta H_f^0(T)]_{\mathrm{reactants}} \tag{5}$$

The heat of formation $\Delta H_f^0$ depends on the bond energy between the atoms of the various compounds. To get as high a combustion temperature as possible, one must select reactants with large (positive) heats of formation and products where the heat of formation is strongly negative. This implies that the bond energies in the propellants shall be as small as possible, while in the products, the bond energies shall be high.

Some typical bond energies for solid propellants and their combustion products are given in Tables 2 and 3. Favorable bonds in propellants are shown in Table 4.

Favorable bonds in combustion products are shown in Table 5.

Two other aspects are important in selecting ingredients for propellant combinations.

To achieve high performance, the combustion should be as complete as possible. Therefore, the propellant shall contain sufficient oxygen to maximize the energy release. Usually, the combustion gases of solid rocket propellants are fuel rich, i.e., in principle more of the fuel could have been oxidized. However, because oxygen has a high molar mass, this increases the mean molar mass of the combustion products. What has to be maximized is the ratio $T_c/\mathcal{M}$ [see Eq. (2)]. Only a detailed evaluation of the combustion process and subsequent expansion through the nozzle, in terms of rocket performance, allows evaluation of the balance between a high

Table 1 Some typical values for $C_p$ in rocket motor combustion gases

| | $C_p$, J/mol·K | | |
|---|---|---|---|
| | 1000 K | 2000 K | 3000 K |
| H | 20.7 | 20.7 | 20.7 |
| $H_2$ | 30.1 | 34.3 | 38.9 |
| HCl | 31.8 | 35.6 | 38.1 |
| $N_2$ | 32.6 | 36.0 | 37.7 |
| CO | 33.1 | 36.4 | 37.7 |
| $CO_2$ | 54.2 | 60.2 | 62.0 |
| $H_2O$ | 41.2 | 51.3 | 56.6 |

Table 2 Typical single covalent bond energies for solid propellants and their combustion products[a]

| | H | C | N | O | Cl | Al |
|---|---|---|---|---|---|---|
| H | 427.2 | 413.0 | 390.8 | 462.8 | 431.4 | 294.6 |
| C | — | 359.8 | 336.4 | 350.6 | 333.9 | 266.5 |
| N | — | — | 158.2 | 238.5 | 191.6 | 322.2 |
| O | — | — | — | 140.6 | 154.4 | 431.4 |
| Cl | — | — | — | — | 242.3 | 430.1 |

[a] Bond energy in kJ/mol.

Table 3 Some typical multiple covalent bond energies for solid propellants and their combustion products[a]

| | | | | | |
|---|---|---|---|---|---|
| O=O | 401.7 | N=O | 401.7 | N=N | 441.4 |
| C=N | 610.4 | C=C | 601.7 | C=O | 680–725 |
| Al=O | 862.7 | — | | — | |
| Al≡N | 728.9 | N≡N | 945.2 | C≡C | 814.4 |

[a] Bond energy in kJ/mol.

Table 4 Favorable bonds in propellants[a]

| | | | | | |
|---|---|---|---|---|---|
| O—O | 140.6 | Cl—O | 154.4 | N—N | 158.2 |
| Cl—N | 191.6 | N—O | 238.5 | — | |

[a] Bond energy in kJ/mol.

Table 5 Favorable bonds in combustion products[a]

| | | | | | |
|---|---|---|---|---|---|
| O—H | 462.8 | H—Cl | 431.4 | Al—O | 431.4 |
| N—H | 390.8 | C—O | 350.6 | C—N | 336.4 |
| Al=O | 862.7 | C=O | 711.3 | — | |
| N≡N | 945.2 | — | | — | |

[a] Bond energy in kJ/mol.

combustion temperature and low molar mass of the combustion products.

The second aspect is the propellant density. This shall be as high as possible, to store as much energy per volume as possible. This is elucidated by Tsiolkovky's equation. This equation may also be written as

$$\Delta v = -I_{\mathrm{sp}} \cdot \log_e(1 - M_p/M_0) \qquad (6)$$

For $M_p/M_0 << 1$, this may be approximated as $\Delta v = I_{\mathrm{sp}} \cdot M_p/M_0$.

$M_p = \rho_p \cdot V_p$, where $\rho_p$ is the propellant density and $V_p$ the volume taken up by the propellant, and so one obtains

$$\Delta v = I_{\mathrm{sp}} \cdot \rho_p \cdot V_p \cdot M_0 \qquad (7)$$

The combination $I_{\mathrm{sp}} \cdot \rho_p = I_\delta$ is called the density impulse. The density impulse is especially important for applications where there is relatively little propellant mass in combination with dry mass, such as for first stages of launchers, boosters, and jet-assisted takeoff devices. It is a typical propellant property. With increasing values of the ratio $M_p/M_0$, the relative importance of $I_\delta$ decreases and the importance of $I_{\mathrm{sp}}$ increases.

### B. Binders

In addition to the previously mentioned thermodynamic characteristics, the binder must have good mechanical properties. This implies a good adhesion between binder, oxidizer, and metal additives.

To optimize performance, the oxygen deficiency of the binder, preferably, shall not be too low.

The first binder that was used was asphalt, in the early and midforties. This was rapidly replaced by the early polyurethanes and later, polyvinyl chlorides. In the early seventies hydroxy terminated polybutadiene (HTPB) emerged as the standard binder for composite propellants. It has excellent mechanical properties and also has a good adhesion with aluminium and ammonium perchlorate (AP), which are the standard ingredients in the composite propellants of today.

An important mechanical characteristic is the glass temperature of a binder. Below this temperature, the binder becomes brittle, and its use at low temperatures becomes difficult. Some typical properties of binders are given in Table 6.

From this table it is seen that HTPB and GAP have the lowest glass points, while GAP and BAMO have the highest heat of formation. PLN and PGN have the lowest oxygen deficiency. As the carbon double bonds in the HTPB backbone cause the incompatibility of HTPB with HNF, the binders GAP and BAMO (like PGN and PLN) are better suited for use with oxidizers like ADN and HNF since they do not have these carbon double bonds in the backbone.

### C. Oxidizers

Like the binders, one has to select oxidizers with low bond energies, i.e., large heats of formation $\Delta H_f^0$. Especially groups with N—O, Cl—N, and Cl—O bonds are of interest in this respect. Substances containing $—NO_2$ and $—NO_3$ groups are commonly used. Examples are ammonium nitrate (AN), RDX, HMX, HNF, and ADN. Oxidizers containing Cl—O bonds are AP, nitronium perchlorate (NP), hydrazinium perchlorate (HP), and hydrazinium di-perchlorate ($HP_2$).

The primary function of the oxidizer is to provide oxygen for the combustion of the fuel. Therefore, it is of utmost importance that the oxidizer releases as much oxygen as possible for the combustion reaction. The stability of the substance is of prime importance for its practical use as an oxidizer in a solid propellant. Stability is not only important during the lifetime of the propellant, but also during the manufacturing of the propellant.

The melting point of an oxidizer is important, because curing of composite propellants usually takes place at elevated temperatures. In addition, a low melting point is often indicative of a low decomposition temperature.

To store as much oxidizer in a volume as possible, the oxidizer density shall be as high as possible. Table 7 lists some of the elementary characteristics of solid oxidizers.

Table 7 shows that HMX has the highest heat of formation, but it has a negative oxygen balance of 21.6%. NP has a positive heat of formation, and a very high oxygen balance. However, this oxidizer is extremely unstable and not suited for use in propellants. ADN and HNF both have a positive oxygen balance, and although the heat of formation is negative, the heat of formation is substantially larger than for AP or AN. The densities of ADN and HNF are also attractive. Only a detailed performance calculation, in combination with a binder, allows establishing which combination of oxidizer and binder gives the best performance. The above considerations may serve as a good guideline to select potential oxidizers and binders.

Table 6 Some typical properties of modern binders[5–13]

| Binder | Chemical formula | $\Delta H_f^0$,[a] kJ/mol | $T_{glass}$, °C | Oxygen balance, %[b] | Density, kg/m$^3$ | Impact sensitivity, Nm |
|---|---|---|---|---|---|---|
| PLN | $[C_5H_9NO_4]_n$ | −334.7 | −25[c] | −114.3 | 1260 | >9 |
| PGN | $[C_3H_5NO_4]_n$ | −284.5 | −35[d] | −60.5 | 1390–1450 | >20 |
| HTPB | $[C_{10}H_{15.4}O_{0.07}]_n$ | −51.9 | −63 | −323.8 | 916 | >50 |
| GAP | $[C_3H_5N_3O]_n$ | 117.2 | −50 | −121.2 | 1300 | 16−>120 |
| BAMO | $[C_5H_8N_6O]_n$ | 413.0 | −39 | −123.8 | 1300 | >20 |

[a] Values apply for $n$ = 1.

[b] The oxygen balance is defined as the ratio of the mass of excess oxygen after a complete conversion of the oxidizer into oxides (with the exception of nitrogen oxides) and the mass of the oxidizer.

[c] By using suitable plasticizers, for PLN glass points as low as −63°C have been obtained.

[d] For PGN the glass point may be lowered substantially by using suitable plasticizers.

Table 7 Some elementary properties of solid oxidizers

| Oxidizer | Molecular formula | Melting/ decomposition temperature, K | $\Delta H_f^0$, kJ/mol | Density, kg/m$^3$ | Oxygen balance, % |
|---|---|---|---|---|---|
| AN | $NH_4NO_3$ | 443 | −365.04 | 1720 | 20.0 |
| AP | $NH_4ClO_4$ | 403 | −296.00 | 1950 | 34.0 |
| HP$_2$[a] | $N_2H_6(ClO_4)_2$ | 443 | −293.30 | 2200 | 41.0 |
| HP[a] | $N_2H_5ClO_4$ | 443 | −177.80 | 1940 | 24.0 |
| ADN | $NH_4N(NO_2)_2$ | 363 | −150.60 | 1820 | 25.8 |
| HNF | $N_2H_5C(NO_2)_3$ | 395 | −72.00 | 1870–1930[b] | 13.1 |
| HP[a] | $NO_2ClO_4$ | 393 | 37.10 | 2220 | 66.0 |
| RDX | $C_3H_6N_6O_6$ | 477 | 70.63 | 1820 | −21.6 |
| HMX | $C_4H_8N_8O_8$ | 548 | 74.88 | 1960 | −21.6 |

[a] HP$_2$, HP, and NP are extremely unstable and not considered suitable as oxidizers.

[b] Based on literature data, measurements at PML-TNO gave a density of 1910 kg/m$^3$.

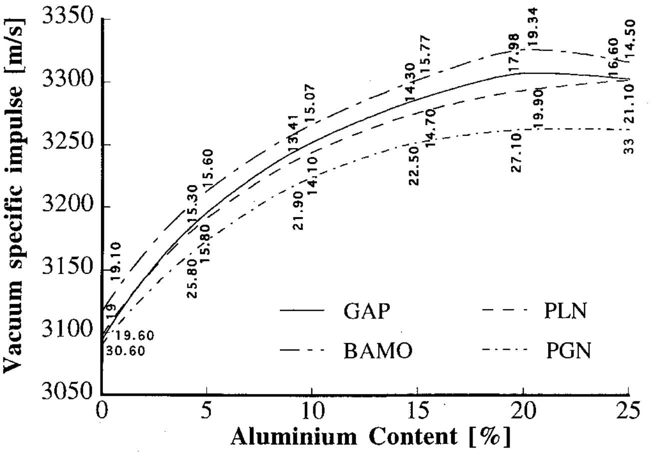

**Fig. 1 Vacuum specific impulse for ADN with BAMO, GAP, PLN, and PGN in relation to aluminium content. The numbers in the graph indicate the percentage of binder. Conditions: $p_c$ = 5 MPa, $\varepsilon$ = 60, equilibrium flow calculations.**

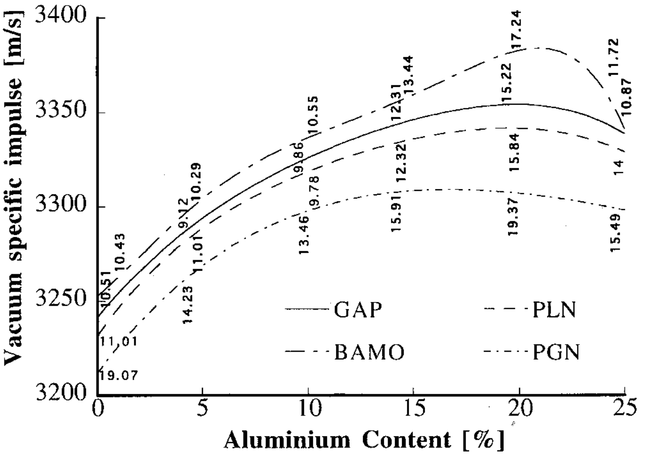

**Fig. 2 Vacuum specific impulse for HNF with BAMO, GAP, PLN, and PGN in relation to aluminium content. The numbers in the graph indicate the percentage of binder. Conditions: $p_c$ = 5 MPa, $\varepsilon$ = 60, equilibrium flow calculations.**

## III. Propellant Performance and Selection of a Propellant Combination

### A. Potential Propellant Performance

The main propellant characteristics with regard to performance are specific impulse $I_{sp}$, and density $\rho$. However, other aspects, such as availability, safe use, ease of handling and manufacturing, and hygroscopicity also play a role. Based upon the results of Sec. II, ingredients with a high heat of formation, a high oxygen balance, and a high density were selected for further evaluation. Metal may be added as an additive, provided the oxygen balance is sufficiently high to warrant the increase in flame temperature.

For high-performance propellants, the following binders and oxidizers are of interest: 1) binders, PLN, PGN, GAP, and BAMO and 2) oxidizers, ADN and HNF.

For the assessment of the performance, the Gordon–McBride code[14] was used. Equilibrium flow calculations were performed for a chamber pressure, $p_c$ = 5 MPa, and an expansion ratio, $\varepsilon$ = 60. These conditions reflect what is customary for apogee boost motors. The results for ADN with the various binders are given in Fig. 1; for HNF with the various binders the results are presented in Fig. 2.

In general, HNF gives about a 1–5% higher specific impulse. However, this data must be regarded as indicative and the differences are probably within the accuracy of the estimate.

Actual propellant performance is affected by finite rate chemistry, nozzle (in)efficiency, and two-phase flow losses. One may estimate these to be in the order of 8%. Taking this 8% loss into account, one might expect overall performances

Table 8 Indicative performance properties of new solid propellant combinations[a]

| | Binder | | | |
|---|---|---|---|---|
| Oxidizer | BAMO | GAP | PLN | PGN |
| ADN | | | | |
| $I_{sp}$, m/s | 3061 | 3043 | 3030 | 3001 |
| $\rho$,[b] kg/m$^3$ | 1895 | 1903 | 1885 | 1888 |
| HNF | | | | |
| $I_{sp}$, m/s | 3112 | 3085 | 3074 | 3044 |
| $\rho$,[b] kg/m$^3$ | 1957 | 1969 | 1959 | 1944 |

[a]Specific impulse based on assumed 8% losses. [b]Estimated.

Table 9 Characteristics of ADN and HNF[5,15,16]

| | ADN | HNF |
|---|---|---|
| Molar mass, kg/kmol | 124.056 | 183.09 |
| Density, kg/m$^3$ | 1820–1840 | 1870–1930 |
| $\Delta H_f^0$, kJ/mol | −150.6 | −72 |
| Melting point, °C | 92.5 | 115–124 |
| DSC-$T_0$, °C | — | 110–124 |
| DSC-energy, kJ/kmol | — | 861 |
| Critical diameter of detonation, mm | 4–8 | — |
| Friction sensitivity, N | — | 20 |
| Impact sensitivity, Nm | — | 3 |
| Toxicity-LD$_{50}$, mg/kg | — | 128 |

of these new oxidizer/binder combinations as given in Table 8.

For all propellant combinations, BAMO yields the largest performance increase. The best practical HTPB/AP/Al propellant (11% HTPB, 18% Al, 71% AP) yields under these conditions, in practice, a specific impulse of 2894 m/s. An interesting feature of PLN and especially PGN is that they allow a high binder fraction in the propellant in combination with high performance.

### B. Characteristics of Potential Ingredients

If no special precautions are taken, the monoclinic crystals of ADN and HNF form needles that make it difficult to obtain a high solid loading. Especially for HNF, which achieves the highest performance at low binder fractions, modification of the crystal shape to more "spherical" or "cubical" crystals is imperative.

HNF is less hygroscopic than ADN, while it also has a higher melting point. Some characteristics of ADN and HNF, as far as known today, are given in Table 9.

As far as available, data for the new binders are summarized in Table 6. Some of these characteristics, like glass point, impact sensitivity, etc., strongly depend on impurities, additives, and plasticizers. As most of these binders are still under development or in a very early stage of application, variation and improvement of these properties may be expected.

### C. Availability of Ingredients

Most of the ingredients for the manufacture of a solid propellant are not (yet) commercially available. ADN has been produced in Russia,[15] but production seems to have ceased there. Until recently there was a small laboratory scale production in the U.S.

HNF is presently produced in three pilot plants: 1) in Japan by Chyugoku Kayaku near Hiroshima, 2) by Hosoya Kakou near Tokyo,[3] and 3) in The Netherlands by APP in Hoogerheide. The latter pilot plant has a capacity of 100 kg/yr, which may be increased to 300 kg/yr.

While the synthesis route for ADN seems to be complex, the synthesis route for HNF is straightforward from hydrazine and nitroform. Hydrazine is produced in Europe by the ESA/DASA hydrazine plant in Trauen, Germany, while nitroform until recently was produced by Rockwell in the U.S. A production of nitroform by SNPE in Europe is foreseen.

For the binders the picture is somewhat different. GAP is commercially available from the 3M company in the U.S. or SNPE in Europe. Also, in Japan a capability for the production of GAP exists.

BAMO seems less developed, and from a performance point of view is the most interesting binder.

PLN recently became commercially available from ICI in Scotland, while PGN is being manufactured at a pilot plant level.

### D. Selection Criteria

From Fig. 2 and Table 8 it is evident that HNF, in combination with one of the new binder systems, may give a substantial performance increase as compared to the presently used HTPB/Al/AP composite propellants. Also, the density of the propellant combinations is attractive.

Safety of handling and manufacturing, toxicity, and compatibility of ingredients must also be considered.

Safety of handling and manufacturing is primarily assessed from the impact, friction, and electrostatic sensitivity, the stability of the ingredients and their compatibility. Although impact and friction sensitivity values for HNF are low, it is believed that they can be improved, while even the present values do not prevent safe handling and propellant manufacturing, e.g., RDX which is commonly used has an impact sensitivity of 5–7.5 Nm.

Toxicity is an important aspect for any new chemical to be handled in industry. Detailed laboratory investigations[17] revealed that HNF is not very toxic in comparison with other ingredients commonly used in solid propellant manufacturing, such as isocyanate curing agents. HNF seems to be a relatively "safe" material, provided the proper handling and safety precautions are taken.

Investigations for GAP indicated that GAP is a nontoxic material. No toxicity data are available for BAMO, PLN, and PGN.

Compatibility between ingredients is important: HNF, for instance, was discovered in the U.S. in the early 1950s. However, although HNF in combination with binders in use in the 1960s gave very good ballistic results, the oxidizer and binder were not compatible. With the new energetic binders, such as GAP, PLN, and PGN, this aspect of the compatibility problem probably has vanished.

### E. Selection of a Propellant Combination

Based upon the criteria above, the combination HNF/GAP has been selected for further evaluation, primarily because of the high performance as compared to the presently used HTPB/Al/AP composite propellant combinations and the availability of HNF and GAP. However, HNF/BAMO and HNF/PGN or PLN also are extremely attractive, and further development work in this direction is envisaged in the United Kingdom.

The optimum performance for an HNF/GAP propellant is achieved with only 15.2% binder. This probably implies too high a solid loading (85%). It is believed, in view of the viscosity of GAP, that a minimum binder fraction of 20% will be necessary. However, even with a binder percentage in the order of 20%, high-performance HNF/Al/GAP composite propellant combinations are feasible. Table 10 gives the estimated propellant density $\rho$ and the vacuum specific impulse $I_{vac}$ as calculated for an equilibrium flow; a chamber pressure $p_c = 5$ MPa and an expansion ratio $\varepsilon = 60$ for propellant combinations with about 20% GAP.

Table 10 also gives the estimated actual propellant performance, assuming an 8% overall loss. The maximum performance in this case is only 5 m/s less than for the best HNF/

**Table 10 Predicted performance for HNF/GAP/Al with about 20% binder**

| Composition | | | Performance | | |
|---|---|---|---|---|---|
| % GAP | % HNF | % Aluminium | $\rho$, kg/m$^3$ | $I_{vac}$, m/s | 92% $I_{vac}$, m/s |
| 20 | 60 | 20 | 1940 | 3348 | 3080 |
| 20 | 55 | 25 | 1980 | 3231 | 2973 |
| 25 | 55 | 20 | 1910 | 3284 | 3021 |

**Table 11 ARIANE 5 performance for injection of HERMES with standard propellant and HNF-based composite propellant**

| Case | Launch mass, Mg | Perigee height, km | Argument of perigee, deg | Payload mass, Mg | Increase in payload mass, kg |
|---|---|---|---|---|---|
| 1 | 739.518 | 69.65 | 0.366 | 22.545 | —— |
| 2 | 741.932 | 68.74 | 2.512 | 24.959 | 2414 |
| 3 | 739.491 | 70 | −0.5 | 22.518 | —— |
| 4 | 741.781 | 70 | 0.0 | 24.808 | 2290 |

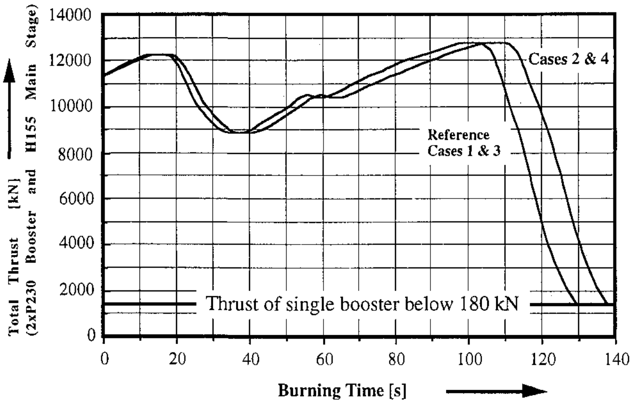

Fig. 3 Thrust profile of central stage of Ariane 5 and solid rocket boosters.

GAP/Al propellant (see Table 8); the density is 29 kg/m$^3$ lower.

## IV. Performance Prediction on Actual Motors

Even with excellent performance and good properties, a new solid propellant is only of interest if it promises substantial improvements over existing propellants. Until now, HNF-based propellants have only been produced and tested at laboratory scale. However, it is of interest to quantify the possible advantages of HNF propellants in existing solid motors to assure the value of the invested effort for its development.

Two typical applications have been analyzed in this article. Both are space related. They do not represent all potential applications of HNF-based propellants.

### A. Ariane 5 Boosters

The Ariane 5 boosters presently use a propellant consisting of AP, Al, and HTPB with a specific impulse of 2660 m/s. Using HNF propellants, an increase in $I_{sp}$ of more than 7% may be achieved, raising the $I_{sp}$ to 2846 m/s.

To assess the effect of this performance gain on the Ariane 5, trajectory calculations have been made to estimate how much more payload could be brought into the HERMES injection point, i.e., a perigee height of 70 km, an osculating apogee height of 512 km that corresponds to a real apogee height of 463 km (considering drag), and an inclination of 28.5 deg.

#### *1. Trajectory and Performance Calculations*

Realistic trajectory calculations can only be made with sophisticated codes. Two codes have been used to make these trajectory analyze: 1) the ESOC ASTROP[18] code and 2) the ESTEC ALTOS[19] code. The ASTROP code is the standard code in use by ESA for trajectory analysis and prediction. The ALTOS code is one of the most advanced trajectory optimization codes presently available. Because these codes have very different structures it was considered useful to make the trajectory analyses with both codes and to compare the results for the following cases:

1) Reference case, standard Ariane 5 concept with the normal Vulcain engine, calculated with the ESTEC ALTOS code.

2) As 1, but with HNF solid propellant, where the thrust profile has been modified to meet the trajectory constraints with the ESTEC ALTOS code.

3) As 1, with the ESOC ASTROP code.

4) As 2, with the ESOC ASTROP code.

The ESOC calculations met all constraints for the Ariane 5 HERMES launch (target orbit, dynamic pressure, heat flux, altitude/velocity, and H155 falldown area), while the ESTEC calculations initially violated the heat flux and the altitude/velocity constraints. Using HNF-based propellant, the thrust profile had to be modified. The increase in specific impulse by 7% leads to a proportional increase of the thrust if the burn time remains constant. This made it difficult to meet all constraints simultaneously, and initially led to inefficient trajectories. To overcome this problem, the burning time of the solid rocket boosters was increased by 7%, in order not to exceed the thrust profile of the reference mission. The resulting thrust profile is given in Fig. 3.

#### *2. Results*

The results of the Ariane 5 performance analyses are given in Table 11. These trajectory analyses demonstrate that the use of HNF-based propellant increases the payload mass by 2290–2414 kg (or ~10%) as compared to the present Ariane 5 performance for a HERMES launch.

The difference in results is believed to come from some nonrespected constraints in the ALTOS code. Without any change in the infrastructure for the booster production, the ARIANE 5 Hermes performance may be increased significantly.

### B. MAGE Booster

The SEP Moteur d'Apogée Géostationaire Europëen (MAGE) is ESA's solid apogee boost motor workhorse for the satellite transfer from the geostationary transfer orbit to the geostationary orbit. Depending on the type (1, 1S or 2), it uses 250–490 kg propellant consisting of AP, Al, and CTPB with a specific impulse varying between 2825–2884 m/s. Using HNF propellants, an increase in $I_{sp}$ of more than 7% may be achieved, raising the $I_{sp}$ to 3021–3090 m/s.

The decrease in propellant mass if an HNF/GAP propellant is used instead of the classical AP/CTPB propellant follows directly from Tsiolkovky's equation [Eq. (1)]. For satellite masses between 700–1200 kg, the required propellant mass (and, hence, the launch mass) decreases by 15–25 kg, or about 5–6%.

As such, this does not seem impressive. However, as the launch cost of a satellite directly depends on the launched mass, the mass advantage of using a more performing propellant may be translated into a reduced launch cost. Taking a launch cost of $18.000/kg, the mass advantages indicated above correspond to $262.000–$444.000. If this amount were paid by the satellite manufacturer to invest into the new propellant to keep the same launch cost, the price of the HNF propellant could be $960/kg higher than for the classical carboxy terminated polybutadiene (CTPB) propellant.

In the ARIANE 5/HERMES case as well as in the MAGE case, HNF-based propellants show very interesting perspectives. Moreover, the performance improvement may be obtained without major changes in the production process already in place today and completely eliminates chlorine pollution, if used in the Earth's atmosphere.

## V. Determination of HNF Characteristics

In view of the promising high performance of HNF/GAP propellants, it was decided to undertake substantial research and development efforts for this family of propellants. A major focus of interest is the HNF itself. A number of preliminary assessment tests have been carried out to determine the main thermodynamic and hazard characteristics of HNF.

### A. Thermodynamic Characteristics of HNF

Some thermodynamic characteristics of HNF are listed in the literature, but they differ to some extent. To obtain better and more complete data on the thermodynamic characteristics of HNF, a number of characterization tests have been performed on HNF: determination of melting point, differential thermal analysis (DTA) and thermogravimetric analysis.

The melting point of HNF listed in the literature[20–22] ranges between 120–123°C. The melting point is related to purity. It is difficult to obtain pure HNF, and so this may explain the scatter in the literature data for the melting point of HNF. The maximum value for the melting point of purified HNF determined during these assessment tests is 124°C. The stability of HNF is also strongly related to its purity. The melting point, therefore, is a first indication of stability.

For the heat of formation, only data from the open literature[22,23] are available; values of $\Delta H_f^0 = -71$ and $-72$ kJ/mol are listed.

DTA measurements on HNF samples (heating rate 10°C/min) gave the following results: a weak exothermic effect at ~109°C with a small maximum at 110°C. This is then followed by an exotherm with a maximum at 134°C, the onset at 136°C of a subsequent exotherm followed by a maximum at 139°C. These results are not completely in agreement with the literature. McHale and Von Elbe[21] using a heating rate of 2°C/min indicate a strong exotherm at a temperature of ~120°C. However, this may well agree with the DTA signals at 134–139°C, as a change to higher values for the exotherms is a well-known phenomenon if higher heating rates are used with the DTA apparatus.

Thermogravimetric analysis of an early sample of HNF in the temperature range between 20–110°C (heating rate 4°C/min) in air indicated that no detectable mass decrease occurs between 20–90°C. In the region between 90–105°C, a very small decrease was noticed (1.4%).

At $T \geq 105$°C rapid decomposition took place with a correspondingly large mass decrease. After the experiment no material could be recovered.

It is believed that the discrepancy between the decomposition temperatures of the early and later samples is caused by impurities in the early HNF samples.

### B. Decomposition Characteristics of HNF

By means of temperature-jump/Fourier transform infra red spectroscopy (T-jump/FTIR) the decomposition behavior of HNF was studied under various conditions.[24] It was found that the thermal decomposition of HNF has three different temperature regions.

In the first temperature region between 25–123°C only preheating of HNF occurs. When the decomposition temperature is reached (~123°C) only one solid product is found by IR spectroscopy; ammonium nitrate ($NH_4NO_3$). This is explained by the slow decomposition of HNF into ANF [$NH_4 \cdot C(NO_2)_3$], which very rapidly decomposes into solid $NH_4NO_3$ and gaseous products.

The second temperature region that can be indicated lies between 123–260°C, where two-phase foam chemistry occurs. In this region the formation of a melt/foam layer on the HNF surface occurs. The following reaction products were identified by IR spectroscopy; ammonium nitroformate (ANF) aerosol, nitroform, hydrazine, $N_2O$, $H_2O$, and CO.

The presence of these products may be explained by the following three reactions:

$$2\text{HNF} \rightarrow 2\text{ANF} + N_2 + H_2 \tag{8}$$

$$\text{HNF (1)} \rightarrow HC(NO_2)_3\text{ (g)} + N_2H_4\text{ (g)} \tag{9}$$

$$2\text{ANF (1)} \rightarrow N_2O + 2CO + 4H_2O + 5/2O_2 + 3N_2 \tag{10}$$

The third temperature region is above 260°C. In this region deflagration of HNF dominates. Looking at the products under these conditions, the formation of $CO_2$ occurs for the first time and is found to be strongly dependent on temperature. The following reaction is proposed to explain the products found:

$$\text{HNF} \rightarrow 2NO + CO_2 + 2H_2O + 3/2N_2 + 1/2H_2 \tag{11}$$

Due to these different temperature regions and the different competing reactions taking place, it is difficult to obtain precise values for the decomposition kinetics of HNF. Decomposition measurements indicate that at ambient pressure and an HNF temperature of 190°C, the decomposition rate is 0.95 mm/s, while at a pressure of 70 bar and an HNF temperature of 400°C the decomposition rate has increased to ~50 mm/s. Indications are that HNF under the investigated conditions decomposes smoothly.

### C. Friction and Impact Test Results

Using a BAM apparatus[30] for the determination of the impact and friction sensitivity, it was found that the results strongly depend on the particle size and shape of the HNF. The purity of the HNF itself and the kind of contaminants also affect the sensitivities. Contaminated HNF showed values for the impact sensitivity <1 Nm, which is too sensitive for use as a propellant ingredient. Purification by recrystallization of the product gave an improvement and impact sensitivity values of 3 Nm have been obtained. The friction sensitivity of pure HNF was found to be 20 N.

### D. Toxicity of HNF

HNF has been investigated for its toxic properties. The acute oral and dermal toxicity were determined[26,27] and the following results were obtained: for the lethal doses for 50% of the test animals ($LD_{50}$) of HNF for dermal toxicity a value ≥2000 mg HNF/kg body weight was found. This means that HNF is a nontoxic material when exposed to via the skin. In an oral toxicity study, an $LD_{50}$ of 128 mg/kg body weight was found; according to the European community (EC) standards this makes HNF a toxic compound.

Also, the effect of HNF on the eyes[28] was investigated. Altogether, it was concluded that HNF is not irritative or corrosive to eyes and skin.

Preliminary mutagenic activity tests[29] (Ames test) showed mutagenic activity in two out of five strains of different salmonella bacteria. For the final determination of the mutagenic activity of HNF, other, more sophisticated, tests will be needed.

### E. Vacuum Thermal Stability (VTS) of HNF

A compound is considered to be thermally stable[23,25] if the gas evolution during 40 h storage under vacuum at 100°C is ≤5 ml/g.

In practice, for HNF, the temperature at which the test is performed cannot be too high due to its decomposition temperature of 123°C. Experiments with HNF in the past indicated that a test temperature of 60°C in combination with a gas evolution less than 5 ml/g during 48 h is acceptable for a preliminary assessment. Later this value was lowered to 3 ml/g.

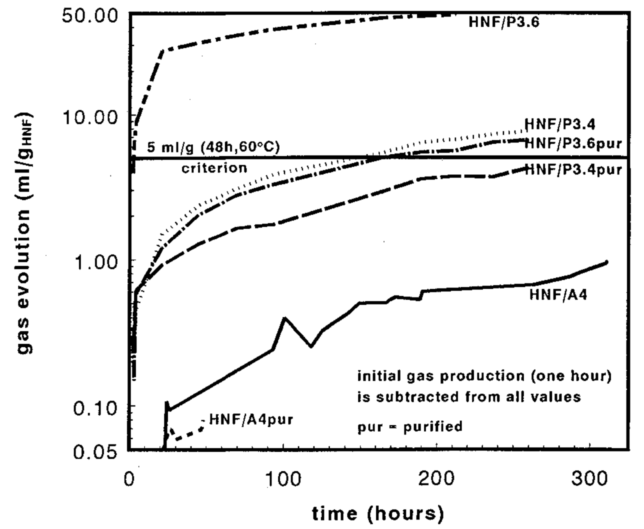

**Fig. 4 VTS measurements at 60°C of different HNF batches; effect of purification.**

As will be shown later, the VTS results of HNF are strongly affected by the purity of the material. Figure 4 shows the effect of purification of raw material with regard to the actual gas evolution. These results show that for safe use of HNF the material in most cases requires additional purification. A number of reasons can be given for the excessive gas evolution of raw HNF. Raw HNF is probably polluted by the solvent(s) used during the production process, causing a gas evolution that is not related to instability or incompatibility, but which results from the evaporation of these solvents. Also, an excess of nitroform or hydrazine within the material will result in excessive outgassing. This explains why additional purification is beneficial. In the past, and especially in the early 1960s, it was found that HNF did not exhibit a good stability. The present work has indicated that stable HNF may be obtained if proper production methods are used. Nevertheless, a number of "stabilizers" have been investigated. In particular: oxalic acid, $MgSO_4$, $CaCO_3$, $MgSO_4$. $ZnCl_2$, diphenyl amine, benzaldehyde, and nitroguanidine. The first two stabilizers improved the stability of "stable" HNF, but had less effect on batches of HNF that displayed lower stability. Their effect on cured HNF propellant was hardly noticeable, and so there was no reason to use stabilizers in this stage of the development.

## VI. Curing of HNF/Al/GAP Propellant

Curing implies a good compatibility with all the ingredients of the propellant in the broadest sense of the word: no unwanted reactions of the oxidizer and no interference in required chemical and physical reactions between ingredients, e.g., curing, wetting, and adhesion.

Incompatibility between HNF and HTPB binder was a major reason why interest in HNF was lost in the 1960s. The observed compatibility problems of HNF with HTPB are attributed to oxidation of the carbon double bonds in HTPB by HNF. Due to this oxidation the binder deteriorates leading to unacceptably low mechanical properties while the HNF decomposition leads to stability problems. To demonstrate the compatibility of HNF with the GAP binder it is essential to obtain proof of concept for this propellant system.

The proof of concept demands the availability of a sufficiently stable, curable, and processable propellant with reasonable mechanical properties. Later in this article the compatibility testing of HNF with the binder components in order to find a good curable HNF-binder system is described.

The binder system that is presently being investigated for the new HNF propellant is based on GAP. GAP does not contain carbon double bonds and is, therefore, less sensitive to oxidation.

However, the compatibility problems observed with HNF are not limited to the HTPB binder. Patents[31,32] also indicate compatibility problems with isocyanates, the commonly used curing agents for HTPB and GAP. Although the mechanism of this incompatibility is unknown, it is believed to be a competitive reaction of the free isocyanate group with the binder and HNF, respectively. For the development of a good binder system the possible incompatibility with isocyanates has to be overcome. For the investigations the following ingredients were used: 1) GAP diol obtained from SNPE (F), with a molar mass, $\mathcal{M} \sim 2000$ kg/kmol; 2) various types of isocyanates: aliphatic, cyclic, and polymeric di-isocyanates, and polyfunctional isocyanates[31–33]; and 3) HNF synthesized at bench scale (300 g/batch) at the TNO Prins Maurits Laboratory.

### A. VTS Test

To determine the compatibility of the ingredients with HNF a VTS test was performed. The preliminary criterion for compatibility of propellant ingredients was also set at less than 5 ml gas evolution per gram material after 48 h at 60°C.

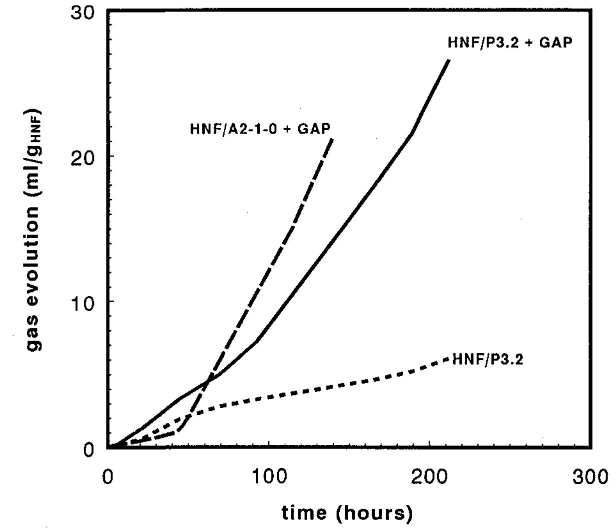

**Fig. 5 Gas evolution in the VTS tests of HNF and HNF + GAP at 60°C.**

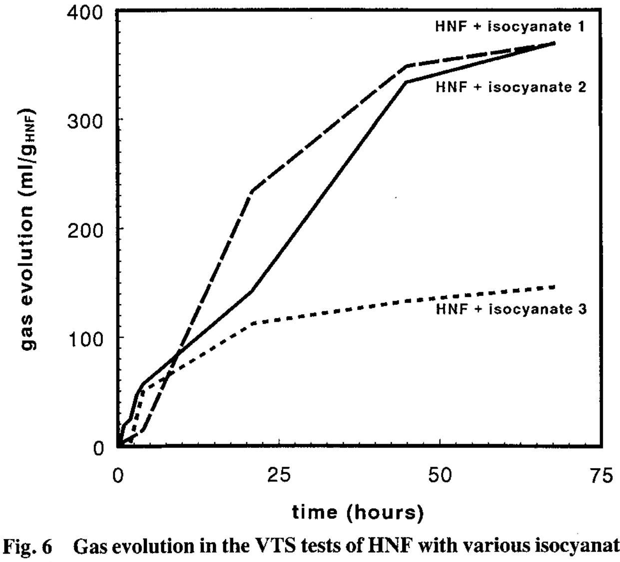

**Fig. 6 Gas evolution in the VTS tests of HNF with various isocyanates at 60°C.**

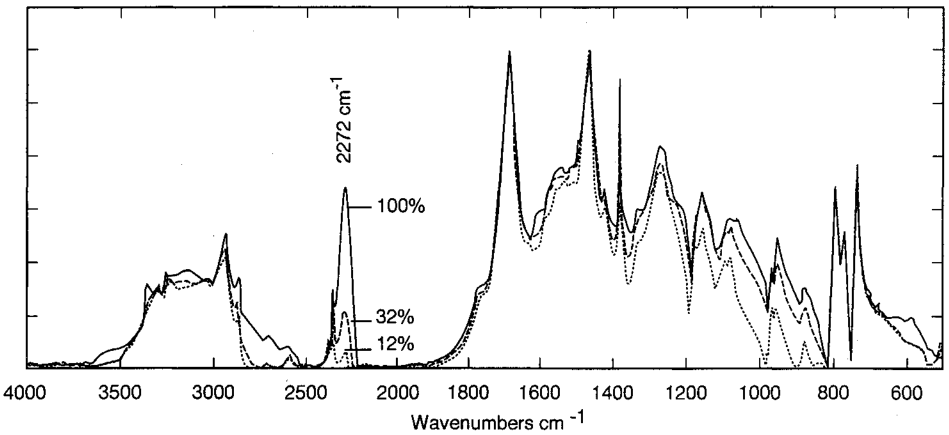

**Fig. 7 IR spectra of mixture of HNF and a typical isocyanate, taken at 0, 19, and 48 h after mixing.**

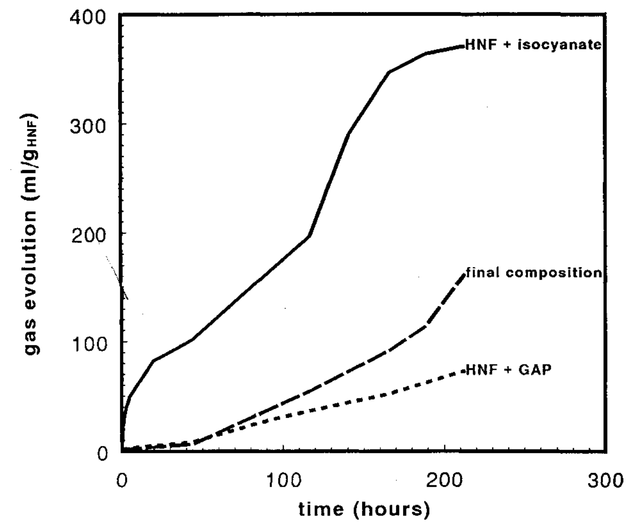

**Fig. 8 Gas evolution in the VTS tests of a cured HNF propellant at 60°C.**

For compatibility testing the HNF was mixed with GAP in a 1:1 mass ratio. For comparison, the gas evolution of pure HNF in the VTS is shown in Fig. 5. The gas evolution of the other pure ingredients is negligible and not shown here.

The results indicate that, although the initial gas evolution of HNF + GAP is acceptable, it is still high.

The compatibility of HNF with isocyanates was tested the same way: 1:1 mass ratios of HNF and the various isocyanates. The VTS results of these mixtures are shown in Fig. 6. The different gas evolutions for HNF + isocyanates are plotted. All tested isocyanates show a poor compatibility with HNF. However, a few remarks have to be made.

1) The HNF production was not yet optimized and since the execution of these tests, the purity and stability of HNF has been improved significantly. It is known by now that the purity of HNF strongly affects its stability.

2) Part of the initial gas evolution may be attributed to the evaporation of solvent adhered to the HNF surface and/or evaporation of any other molecules with low molecular mass, and hence, is not part of any incompatibility reaction.

Since the VTS results indicate a reaction between HNF and isocyanates, IR-spectroscopy was applied to verify this. The pure isocyanates all have a very distinct absorption peak at 2270 $\mathrm{cm}^{-1}$ due to the reactive isocyanate (—N=C=O) group. This group is the most likely to react with HNF and changes in this group will directly affect the intensity of this absorption peak. When several IR spectra of a HNF–isocyanate mixture are taken over a certain period, the change in intensity is a measure for the change in concentration of this reactive isocyanate group. The spectra taken at 0, 19, and 48 h, respectively, after mixing, are shown in Fig. 7.

The spectra show a strong decrease in the isocyanate absorption peak from 100 to 12%. This implies that the tested isocyanate reacts nearly completely with HNF within two days at ambient temperature.

A reference sample of isocyanate with potassium sulphate, an inert solid, did not show any reduction in the intensity of the —N=C=O peak over time.

A possible reaction mechanism is a hydrogen transfer from the HNF to the nitrogen in the —N=C=O group. This reaction resembles the well-known reaction of isocyanates with amines.[34] This would destabilize the HNF leading to decomposition (gas evolution in the VTS), and would reduce the intensity of the —N=C=O absorption peak in the IR spectrum. This mechanism explains, at least qualitatively, the observed phenomena.

It is assumed that once the isocyanate group has reacted with the hydroxyl group of GAP, it will lose its reactivity with HNF. It is known that the urethane group is not reactive towards amines or alike compounds. Evidence for this is only preliminary, but a cured HNF propellant sample showed a significantly reduced gas evolution in the VTS compared to the isocyanate + HNF mixture as indicted in Fig. 8 by the line "final composition."

### B. Small-Scale Processing Trials

In addition to the chemical reaction between isocyanates and HNF, other effects might occur. To verify this, small-scale propellant mixtures have been prepared and judged with respect to potlife, curing behavior, and qualitative mechanical properties. Quantitative mechanical testing has not yet been performed because the available amount of propellant was insufficient to perform these tests.

All the mixtures consisted of HNF, GAP, isocyanate, and a curing catalyst system. The following parameters were varied: 1) type and amount of isocyanate; 2) mixing and curing temperature; 3) type and amount of curing catalysts; 4) purity, particle size and morphology of the HNF; and 5) application of "coating" agents.

All the variations were aimed at favoring the isocyanate + GAP curing reaction and inhibiting the isocyanate–HNF reaction. The identified optimum procedure lead to a cured propellant with acceptable properties and stability.

Observations from these tests are as follows:

1) Initial tests showed thickening of the mixture explained by an immobilization of the isocyanates molecules at the HNF surface.

2) Initial tests showed short potlifes due to this "thickening" of the mixture.

3) Treatment of the HNF with coating agents to prevent reactions on the HNF surface did not show any improvement.

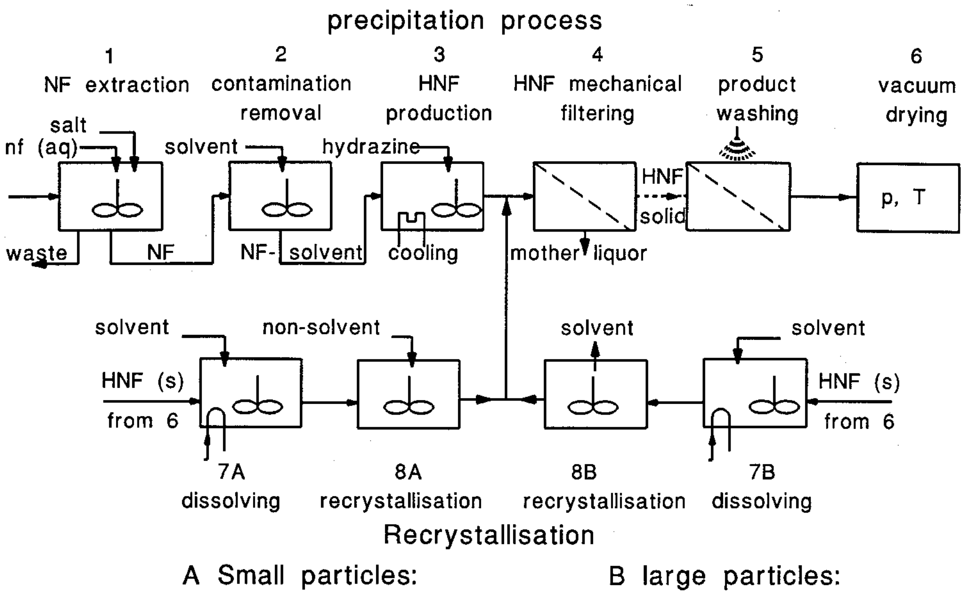

**Fig. 9 Schematic production process (bench scale and pilot plant scale).**

4) By using the various isocyanates, curing catalysts, and curing conditions, a large variation in curing results was obtained. It ranged from noncured products to products with voids until good rubber-like samples.

5) The purity, particle size, and morphology of the HNF was again shown to have a strong effect on the curing and the final propellant properties.

6) The final composition was a rubbery product with a potlife of 1 h and good curing within 2 days.

The overall compatibility of HNF with the various binder ingredients is not yet satisfactory. However, the purity and morphology of the HNF play an important role in this, and recent HNF production batches show further improvement of the HNF stability. Moreover, the propellant is of sufficient quality to perform initial ballistic tests with cured propellant in the near future.

## VII. Manufacturing of HNF

Production of HNF is a simple acid-base reaction between nitroform and hydrazine. However, handling of the raw materials with respect to the hazardous properties such as toxicity, carcinogenicity, reactivity, and explosivity requires special precautions, equipment, and infrastructure. In addition, possible contamination of the ingredients may lead to low-quality HNF due to parallel side reactions or successive reactions with the contaminants present during production. Finally, deviation from the stoichiometric ratio between the two raw materials may also lead to rapid deterioration of the HNF. This implies that an excellent quality control of the ingredients and of the manufacturing process is required to obtain good quality and stable HNF.

### A. Manufacturing Process

In 1988 the Prins Maurits Laboratory TNO started the investigation of a reliable and safe production process for HNF. Initially, the process was developed on laboratory scale with a yield of about 10 g/batch. Subsequently, this production method was scaled up to 300 g/batch in a bench-scale process for which a patent application[35] has been filed.

The formation reaction of HNF according to

$$N_2H_4(l) + HC(NO_2)_3(l) \rightarrow N_2H_5^+\,{}^-C(NO_2)_3(s)$$

$$\Delta H^0_{\text{reaction}}(298) \sim -84 \text{ kJ/mole}$$

is a precipitation reaction. Because the reaction is exothermic, the process vessel must be thoroughly cooled. The temperature of the vessel is kept below 5°C in order not to exceed the flash point temperature of the reaction medium ethylene di-chloride (EDC).

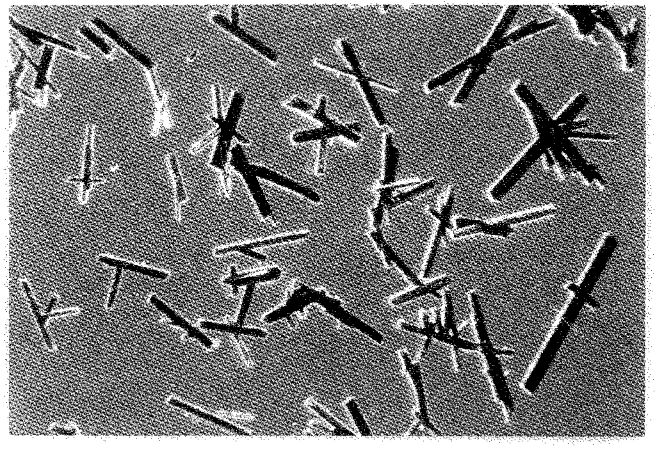

**Fig. 10 Needle-shaped HNF crystal after recrystallization ($\langle x \rangle = 640 \pm 50\ \mu m$).**

The process to obtain HNF may be split into six consecutive process steps (Fig. 9). Steps 1 and 2 are extraction steps: step 1 to extract nitroform from the aqueous phase into EDC. This is achieved by means of a salt displacement extraction (sodium chloride is added to the aqueous nitroform solution to force nitroform out of the water phase), and step 2 is for removing possible contaminants present in the extract.

Step 3 is the actual production step of HNF. HNF is precipitated by addition of liquid hydrazine to the nitroform/EDC solution.

In step 4 the HNF/EDC slurry is filtered through a mechanical filter where after (step 5) the filter cake is washed in the mechanical filter with a washing liquid.

Afterwards (step 6) the HNF crystals are dried in a vacuum oven at elevated temperatures at subatmospheric pressure.

Steps 5 and 6 are important steps to obtain good-quality HNF. Washing the crystals is needed to remove contaminants and excess of nonreacted nitroform or hydrazine. Drying is crucial to remove remaining nitroform and solvent that might have been adsorbed to the crystals. These two process steps

Table 12 Analysis results for various HNF batches

| HNF batch code | HNF purity acid based, % | HNF purity hydrazine based, % | VTS 48 h 60°C, ml/g | % NaCl or Cl-based, % | Yield based on nitroform: Extraction, % | Yield based on nitroform: Precipitation recrystallization, % | Melting point, °C |
|---|---|---|---|---|---|---|---|
| Raw production batches | | | | | | | |
| 5-0-0 | 99.80 | 98.16 | 0.90 | 0.022 | 77 | 81 | 117.6 |
| 4-0-0 | 100.36 | 97.35 | 0.31 | <d.l.[a] | 71 | 85 | — |
| 3-0-0 | 99.92 | 98.01 | 0.64 | <d.l. | 74 | 77 | 120.4 |
| 2-0-0 | 98.65 | 99.42 | 2.86[b] | 0.141 | 67 | 99 | —— |
| Recrystallized batches | | | | | | | |
| 2-1-0 | 100.09 | 99.99 | 0.79 | 0.195[c] | NA[d] | 83 | 123.2 |
| 2-0-1 | 100.33 | 99.84 | 0.61 | <d.l. | NA | 47[e] | 123.2 |

[a] <d.l. = Below detection limit which is lower than 0.01%.
[b] Drying of HNF 2-0-0 started only after 6 days instead of directly after production of the batch.
[c] The increase of NaCl content is probably due to the fact that NaCl serves as nucleus for HNF crystallization.
[d] NA = not applicable.
[e] Because of the small batch size recrystallized the yield is rather low due to relatively high processing losses.

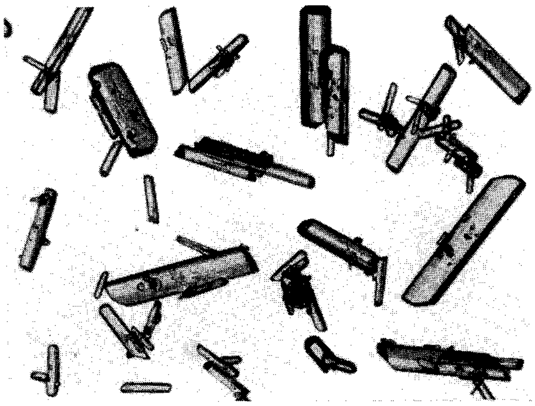

Fig. 11 Recrystallized HNF with $l/d$ ratios 4–5 ($\langle x \rangle$ = ~500 $\mu$m).

prevent any reaction after the production of HNF and as such stabilize the final product.

In addition, two recrystallization methods were developed on bench-scale size. This was necessary to improve the purity of the raw HNF and to be able to obtain different sizes of HNF crystals. Small particle size HNF ($\langle x \rangle \sim 20$ $\mu$m) (the mean dimension, $\langle x \rangle$, is volume based) is produced by dissolving HNF where after HNF is recovered by adding a nonsolvent to the solution (steps 7A and 8A in Fig. 9). The recrystallized HNF is filtered, washed, and dried (steps 4–6).

Large particle size HNF ($\langle x \rangle \sim 200$ $\mu$m) is generated by using a recrystallization process based on evaporation of the solvent in which HNF is dissolved (steps 7B and 8B). Again, the obtained crystals are filtered, washed, and dried (steps 4–6). Recrystallizing HNF leads to a high-purity product and although different particle sizes can be obtained, the shape of the particles still leaves to be desired. As can be seen in Fig. 10 the HNF crystals have a tendency towards needle-shaped growth.

This needle shape is not desirable for propellant production. Needle-shaped HNF seems to be more sensitive to impact and friction and is not desirable for propellant production. For the research and development, to manipulate crystal shape, to improve the controllability of the HNF crystal size distribution, and to develop the final propellant composition, substantial amounts of HNF are required. Already some improvements, see Fig. 11, have been made to reduce the length over diameter ratio ($l/d$) to 2–5 for both large and small crystal sizes.

After technical problems, like batch-to-batch variations and product quality, had been investigated and solved with the bench-scale equipment, a pilot plant with a capacity of 30–300 kg/year was designed and built to satisfy the increased demand of HNF.

Figure 9 shows the consecutive steps of the three processes as operated with both bench scale and pilot plant; precipitation and two recrystallization methods. The process steps are batchwise operated.

This pilot plant allows the production of about 3–5 kg (raw) HNF/batch with an average particle size of $\langle x \rangle \sim 400$ $\mu$m. After recrystallization, the obtained average particle size is $\langle x \rangle \sim 40$ $\mu$m (small) or $\langle x \rangle \sim 500$ $\mu$m (large), depending on the recrystallization method. Production of raw HNF showed minor batch-to-batch variations (see below). The quality of HNF from the pilot plant before recrystallization is comparable to the quality of HNF batches produced with the bench scale after recrystallization.

## B. Quality Control

The ingredients, hydrazine and nitroform, are submitted to a thorough incoming goods inspection for purity and contaminants. During the development of the production process various analytical techniques to verify and control the quality of HNF have been investigated and verified. This resulted in a set of elementary tests to establish the quality of the produced HNF immediately after production. One of the drawbacks of these analyses is that the purity of HNF is not directly measured. The hydrazine content and the acid content (nitroform + HNF + acid contaminations) are determined separately to derive the purity of HNF. Improved analytical techniques are under investigation.

Table 12 shows the results from four raw HNF batches and two batches (HNF-2-1-0 and HNF-2-0-1) recrystallized from raw batch HNF-2-0-0. In this table two HNF purity percentages are presented. One is based on the acid number, where all acid groups are calculated to originate from HNF. The other one is based on the total amount of hydrazine present in HNF. The pilot plant was designed to deliver HNF with a purity better than 97% based on hydrazine. The maximum value for the VTS was set at 3 ml/g HNF. The sodium chloride, introduced in the first extraction step, shall not exceed 0.05% in the final product. The yields are calculated with respect to nitroform. The first column represents the yield of the extraction of nitroform, the latter yield depicts the yield of the HNF precipitation step or the recrystallization step. The melting point is indicative for purity.

## C. Future Production and Industrialization

After careful evaluation of the different steps in the production path for HNF, large-scale production of HNF might very well be carried out continuously. Whether continuous production is commercially interesting largely depends on the demand for HNF.

With the current methods of extraction of nitroform, low yields are obtained (~72%), and contamination with sodium chloride may take place. Initial tests show that nitroform can be extracted by means of liquid–liquid extraction with yields reaching 94% or even higher if continuous counter column liquid–liquid extraction is used.

Production of HNF in a continuous crystallizer equipped with classified product removal (only removing particles with a specific size) and recycling of fines (returning too small particles to the crystallizer), together with the continuous liquid–liquid extraction is an attractive option for large-scale production of HNF.

Such a production process may lead to significant cost reductions in the production of HNF. When large-scale production of HNF is required, the costs of both nitroform and hydrazine may also drop considerably. In fact, the production of nitroform may be carried out continuously and be a direct input for the HNF production. This leaves out several intermediate process steps such as dissolving nitroform in water for transportation and retrieving nitroform from water for production of HNF. Figure 12 is a schematic process layout of such a continuously operated HNF production plant. In this case a continuous nitroform extraction step is also displayed, but the plant might also be fed directly from the output of a nitroform production unit.

## VIII. Determination of Characteristics of HNF/Al/GAP Propellant

### A. Friction and Impact Test Results

Friction and impact sensitivity of HNF and HNF/Al/ (uncured) GAP mixtures may be compared with more conventional propellant formulations. The results (Table 13) show that the values for impact and friction sensitivity of HNF-based propellants, although somewhat lower than those for AP- and AN-based propellants, are acceptable for practical use.

To obtain maximum performance the production of a castable solid propellant would require a composition of about 15% GAP, 20% Al, and 65% HNF (see Fig. 2). However, as this implies too high a solid loading for GAP, a good composition for development purposes may be obtained by 60% HNF, 20% Al, and 20% GAP (by weight). Even with this solid loading of 80%, the availability of multimodal HNF is mandatory. With the available needle-shaped bimodal HNF crystals, a maximum solid loading of about 75% could be obtained for a castable solid propellant. In addition, a suitable curing system for HNF/GAP was not yet available at the time of the initial tests. A pressed propellant with composition as indicated above is not hampered by these restrictions. In the following results of experiments with pressed HNF/Al/GAP, propellant mixtures are reported that were obtained in a period when neither HNF particles leading to a high packing density nor a suitable curing system were available. For the pressed propellant, bimodal, needle-shaped HNF (33.3% coarse, i.e., $\langle x \rangle$ = 150–200 $\mu$m and 66.7% fine, i.e., $\langle x \rangle$ = 10–20 $\mu$m) was used.

### B. Compatibility

The compatibility of HNF with (uncured) GAP and aluminium has been determined by VTS tests. The results are shown in Table 14. The criterion for compatibility in a propellant combination has arbitrarily been set to a gas evolution <5 ml/g/sample during 48 h at a temperature of 60°C.

**Table 13 Sensitivity data of HNF and HNF (pressed) propellant mixtures in comparison to typical AP and AN based propellant systems**

| Composition | Impact sensitivity, Nm | Friction sensitivity, N |
|---|---|---|
| HNF | 7.5 | 24 |
| First batch | | |
| 60% HNF / 20% Al / 20% GAP | 3 | 30 |
| Later batches | | |
| 59% HNF / 21% Al / 20% GAP | 15 | 24 |
| Literature[36] | | |
| AP/Al based propellants | 15–25 | 30 |
| AN/GAP/BDNPA-F | 15–25 | >360 |

**Table 14 Compatibility of HNF with GAP and aluminium**

| Composition, by weight % | Gas evolution at 60°C after 48 h, ml/g |
|---|---|
| HNF | 1.4 |
| 50% HNF + 50% GAP | 4.0 |
| 60% HNF + 20% GAP + 20% Al | 3.9 |

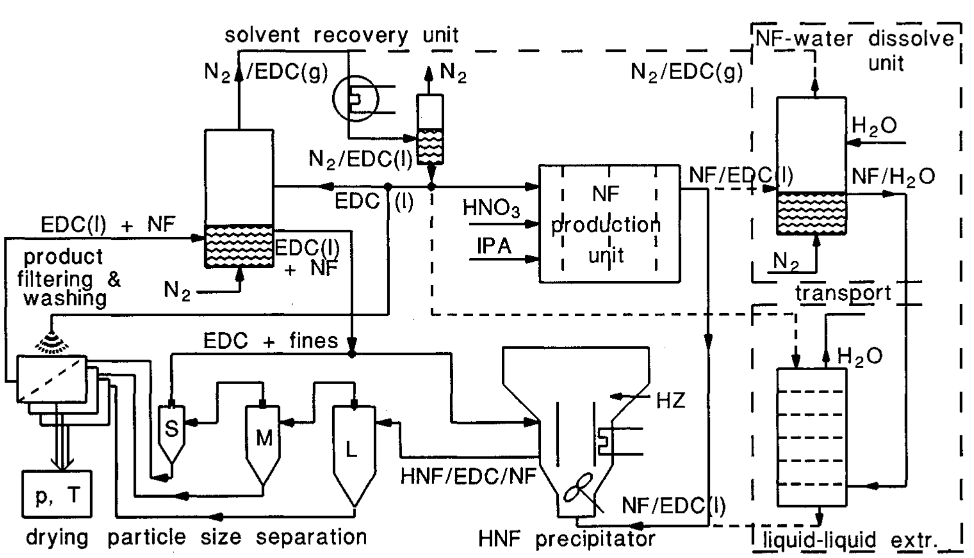

Fig. 12 Schematic diagram of a continuous HNF production plant.

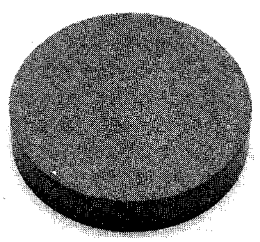

Fig. 13 Pressed HNF/Al/GAP propellant sample.

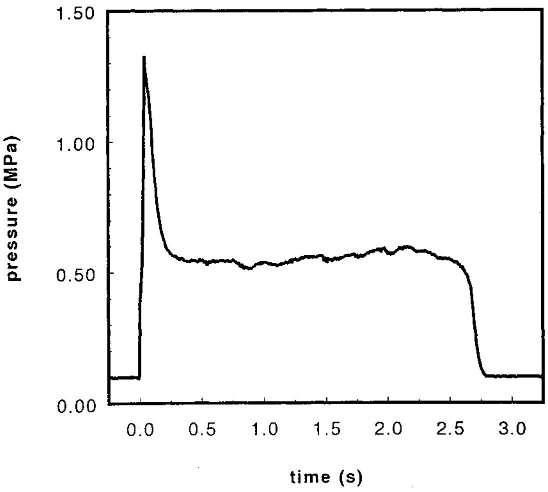

Fig. 14 Typical pressure history of pressed HNF/Al/GAP propellant at low pressure.

### C. Performance Characteristics

Circular disks of pressed propellant [o.d. 50 mm, web thickness ~10 mm (see Fig. 13)] were manufactured for ballistic characterization in a so-called $L^*$ burner (i.d. 100 mm, throat diameters ranging between 5–11 mm). In some cases several (up to four) disks were mounted together. In these cases the o.d.'s of the disks were adapted. An inhibitor was applied at the circumference of each propellant disk before testing, resulting in a cigarette-burning grain. As a result of the high amount of solid matter ($Al_2O_3$) in the combustion product gases, nozzle clogging and nozzle erosion problems were encountered during testing. The use of molybdenum alloy throat inserts eliminated the latter problem, whereas the use of larger throat diameters made the testing less susceptible to nozzle blockage. These initial tests with pressed propellant disks revealed the following:

1) HNF-based propellants are easily ignitable.

2) At low pressures (0.1–1 MPa), the combustion of aluminium is poor, resulting in relatively low $c^*$ values (being ~1200 m/s as compared to predicted value of 1631 m/s at a pressure of 0.5 MPa). Substantial amounts of unburned aluminium were found in the combustion chamber after each low-pressure test. Combustion experiments show smooth, steady-state pressure histories (Fig. 14).

3) At higher pressures, combustion pressures were transient. Values for the characteristic velocities determined from the pressure time traces are close to the predicted ones ($c^*$ ~ 1590 m/s as compared to the theoretical value of $c^* = 1667$ m/s at 5.1 MPa).

4) The observed burning rates are high; at 5.5 MPa, the burning rate exceeds 30 mm/s (Fig. 15).

5) The observed high burning rate and high-pressure exponent agree very well with earlier results from work by ESSO and Thiokol. Both companies report pressure exponents of 0.81–0.83.[37]

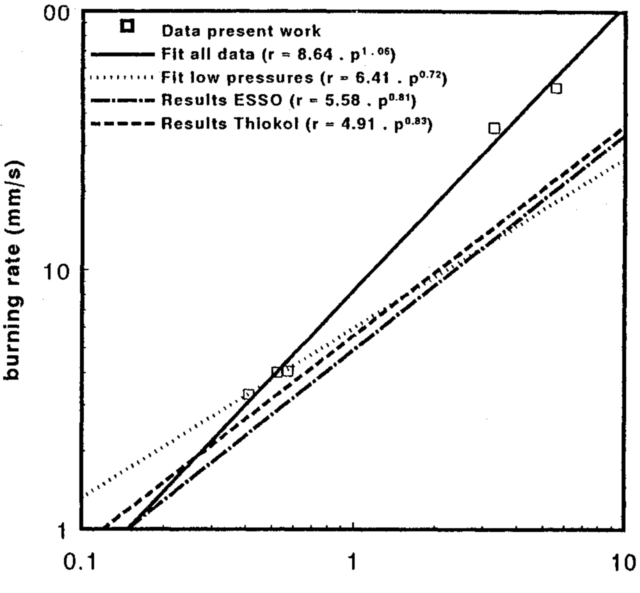

Fig. 15 Burning rate of HNF propellants.

When interpreting these results, it should be kept in mind that these were initial tests with pressed, and not cured, propellant. The experiments confirmed the expected high-performance values, while the burning rate exponent at high pressures agreed with earlier measurements for HNF/HTPB propellants by ESSO and Thiokol. Therefore, the high burning rate exponent seems to be a property of HNF-based propellants. On the other hand, because of the porous nature of pressed propellants, care has to be taken in extrapolating these results to actual, properly cured propellants.

## IX. Conclusions

Performance calculations reveal that a new propellant, based on HNF as an oxidizer and GAP as a binder, is extremely attractive and yields large performance gains.

Laboratory production of HNF demonstrated that a good-quality product with interesting characteristics can be produced safely. Once the initial tests confirmed the expected increase in performance, a pilot plant has been built to supply HNF in sufficient quantities for research and preliminary development.

Combined with GAP, HNF gives a curable propellant with a high burning rate. Still, large efforts are required to obtain fully developed propellants. Several aspects like HNF particle size and shape, curing with GAP, burning rate modification, mechanical properties, combustion properties, and combination with different binders still require substantial research and development efforts.

In the near future, additional rocket engine tests will be performed to demonstrate the properties and potential of the future propellants based on HNF. From the results of the work performed until now the remaining difficulties do not appear insurmountable and the future prospects with regard to possible applications are encouraging.

The increase in specific impulse leads to a marked increase of the performance of solid propellant boosters or apogee boost motors, which directly translates into substantial economic benefits. In addition, the propellants are much less polluting than any of the existing high-performing composite solid propellants available today.

## Acknowledgments

This work was performed under harmonized contracts from the European Space Agency, and The Netherlands Agency for Aerospace Programs, Contracts 7234 and 9007.

## References

[1]Klager, K., "Polyurethanes, the Most Versatile Binder for Solid Composite Propellants," AIAA Paper 84-1239, June 1984.

[2]Mul, J. M., Korting, P. A. O. G., and Schöyer, H. F. R., "A Search for New Storable High-Performance Propellants," *ESA Journal*, Vol. 14, 1990, pp. 253–270.

[3]Kubota, N., private communication, 1994.

[4]Cornelisse, J. W., Schöyer, H. F. R., and Wakker, K. F., *Rocket Propulsion and Spaceflight Dynamics*, Pitman, London, 1979.

[5]Mul, J. M., Gadiot, G. M. H. J. L., Meulenbrugge, J. J., Korting, P. O. A. G., Schnorhk, A. J., and Schöyer, H. F. R., "New Solid Propellants Based on Energetic Binders and HNF," AIAA Paper 92-3627, July 1992.

[6]Campbell, D., Cumming, A. S., and Marshall, E. J., "Development of Insensitive Rocket Propellants Based on Ammonium Nitrate and PolyNimmo," Internal Paper ICI-Explosives, Stevenson, and DRA, Sevenoaks, England, UK, 1994.

[7]Marshall, E. J., and Cumming, A. S., "A Study of the Compatibility, Sensitiveness and Plasticisation of PolyNIMMO and Its Mixes," Propulsion Technology Meeting, Defense Research Establishment Valcartier, Quebec, Canada, May 1994.

[8]Miyazaki, T., and Kubota, N., "Energetics of BAMO," *Journal of Propellants, Explosives and Pyrotechnics*, Vol. 17, No. 1, 1992, pp. 5–9.

[9]Willer, R. L., and Day, R. S., "Poly Glycidyl Nitrate, Revisited," *Proceedings of the ADPA Symposium on Compatibility and Processing*, American Defense Preparedness Association, VA, Oct. 1992, pp. 257–269.

[10]Bagg, C., Desai, H., Leeming, W. B. H., Paul, N. C., Paterson, D. H., and Swinton, P. F., "Scale-Up of PGN Manufacture, Process Development and Assessment," *Proceedings of the ADPA Symposium on Compatibility and Processing*, American Defense Preparedness Association, New Orleans, LA, 1992, pp. 335–348.

[11]Debenham, D., Leeming, W. B. H., and Marshall, E. J., "Application of Poly-Nimmo in Composite Gun Propellants," *Proceedings of the 21st International Annual Conference of ICT*, ICT, Karlsruhe, Germany, 1990, pp. 53-1–53-16.

[12]Wardle, R., "Technical Data Sheet for Poly(Bis(Azidomethylene)Oxetane)," Thiokol Corp., Utah, 1991.

[13]Stewart, M. J., Colclough, E., Golding, P., Millar, R., and Paul, N. C., "Novel Energetic Monomers and Polymers Prepared Using $N_2O_5$ Chemistry," *Proceedings of the ADPA Symposium on Compatibility and Processing*, American Defense Preparedness Association, VA, 1989, pp. 234–240.

[14]Gordon, S., and McBride, B. J., "Computer Program for Calculation of Complex Chemical Equilibrium Compositions, Rocket Performance, Incident and Reflected Shocks, and Chapman–Jouguet Detonations," NASA SP-273, 1971, revised database version 1989.

[15]Pak, Z., "Some Ways to Higher Environmental Safety of Solid Rocket Propellant Application," AIAA Paper 93-1755, June 1993.

[16]Van Lit, P. J., "Specification Sheet HNF," Aerospace Propulsion Products, WP 3100 CCN#3 Issue 1, Rev. 1, Hoogerheide, The Netherlands, March 1994.

[17]Meulenbrugge, J. J., and Mul, J., "Toxicity of GAP and HNF," Aerospace Propulsion Products/Prins Maurits Lab. TNO, WP 600 Summary Rept., Hoogerheide/Rijswijk, The Netherlands, 1992.

[18]Bartholomew-Biggs, M. C., Bartholomew-Biggs, L., Christianson, B., Parkhurst, S., and Dixon, L. C. W., "Advanced Trajectory Optimisation Techniques," ESOC Contract 9330/91/D/MD, Final Rept., Univ. of Hatfield, Hertfordshire, England, UK, Oct. 1992.

[19]Buhl, W., Ebert, K., and Herbst, H., "Optimal Ascent Trajectories for Advanced Launch Vehicles," AIAA Paper 92-5008, Dec. 1992.

[20]Schmidt, E. W., *Hydrazine and Its Derivatives; Preparation, Properties, Applications*, Wiley, New York, 1984.

[21]McHale, E. T., and Von Elbe, G., "The Deflagration of Solid Propellant Oxidizers," *Combustion Science and Technology*, Vol. 2, 1970.

[22]Koroban, V. A., Smirnova, T. I., Barishova, T. N., and Svetlov, B. S., "Kinetics and Mechanism of Thermal Decomposition of Hydrazine Trinitromethane," *Inst. D. I. Mendeleeva*, Vol. 104, 1979, pp. 38–44 (translated from Russian).

[23]Sarner, S. F., *Propellant Chemistry*, Reinhold, New York, 1966.

[24]Williams, G. K., and Brill, T. B., "Thermal Decomposition of Energetic Materials 67. Hydrazinium Nitroformate (HNF) Rates and Pathways Under Combustionlike Conditions," *Combustion and Flame* (to be published).

[25]Anonymous, "Description of Tests Used for the Qualification of Explosive Materials for Military Use," NATO, International Staff Defence Support Div., Allied Ordnance Publication, AOP 7, Brussels, Belgium, 1991.

[26]Prinsen, M. K., "Acute Oral Toxicity Study with Hydrazinium Nitroformate (HNF) in Rats," TNO Nutrition and Food Research, V91.140/200060, Zeist, The Netherlands, June 1991.

[27]Prinsen, M. K., "Acute Dermal Irritation/Corrosion Study with Hydrazinium Nitroformate (HNF) in Albino Rabbits," TNO Nutrition and Food Research, V91.142/200061, Zeist, The Netherlands, April 1991.

[28]Prinsen, M. K., "Acute Eye Irritation/Corrosion Study with Hydrazinium Nitroformate (HNF) in Albino Rabbits," TNO Nutrition and Food Research, V91.141/200069, Zeist, The Netherlands, April 1991.

[29]Blijleven, W. G. H., "Examination of Hydrazinium Nitroformate (HNF) for Mutagenic Activity in the Ames Test," TNO Nutrition and Food Research, V91.204, Zeist, The Netherlands, July 1991.

[30]Anon., "Recommendations on the Transport of Dangerous Goods, Tests and Criteria," 2nd Ed., United Nations, New York, 1990.

[31]Haury, V. E., and Low, G. M., "Hydrazinium Nitroformate Propellant with Saturated Hydrocarbon Binder," U.S. Patent 3,708,359, 1973.

[32]Reed, R., Jr., "Propellant Binder Cure Catalyst," U.S. Patent 4,379,903, 1992.

[33]Tokui, H., Saitoh, T., Hori, K., Notono, K., and Iwama, A., "Synthesis and Physico-Chemical Properties of GAP and the Application of GAP/AN Based Propellants to a Small Motor," *Proceedings of the 21st International Annual Conference of ICT*, Institut für Chemische Technologie, Karlsruhe, Germany, 1990, pp. 7-1–7-14.

[34]Oertel, G., "Poly-Urethane Handbook," Hanser Verlag, Munich, Germany, 1985.

[35]Zee, F. W. M., Mul, J. M., and Hordijk, A. C., "Method of Preparing Hydrazine Nitroform," International Patent Application no. PCT/NL93/00230, Octrooiraad, Rijswijk, The Netherlands, Nov. 1993.

[36]Lessard, P., Druet, L., Villeneuve, S., and Thiboutot, S., "Development of a Minimum Smoke Propellant Based on GAP and Ammonium Nitrate," *AGARD Conference Proceedings*, CP 511, AGARD, Loughton, England, 1992, pp. 12-1–12-5.

[37]Flanagan, J. E., private communication, Rockwell International, Rocketdyne Div., Los Angeles, CA, 1989.